Acta Polytechnica CTU Proceedings **33**:411–416, 2022
https://doi.org/10.14311/APP.2022.33.0411

Published by the Czech Technical University in Prague

PHYSICAL PROPERTIES OF PORTLAND CEMENT BASED CONCRETE EXPOSED AT A DEPTH OF 3520 M IN THE NANKAI TROUGH

Shun Nomura[a,*], Takafumi Kasaya[b], Yuki Sakoi[c], Hisashi Fukada[d], Akira Matsumoto[e]

[a] *Japan Agency for Marin-Earth Science and Technology, Research Institute for Value-Added-Information Generation, Center for Mathematical Science and Advanced Technology, 3173-25 Showa-machi Kanazawa-ku Yokohama-city Kanagawa, 236-0001, Japan*

[b] *Japan Agency for Marin-Earth Science and Technology, Research Institute for Marine Resources Utilization, Submarine Resources Research Center, 2-15 Natsushima-cho Yokosuka-city Kanagawa, 237-0061, Japan*

[c] *Hachinohe Institute of Technology, Faculty of Engineering, Department of Civil Engineering and Architecture, 88-1, Obiraki, Myo, Hachinohe, Aomori, 031-8501, Japan*

[d] *Fudo Tetra Corporation, Geo-Technical division, 7-2 Nihonbashi Komai-cho Chuou-ku, Tokyo, 103-0016, Japan*

[e] *Fudo Tetra Corporation, Technical Research Institute, 2-7 Higashi Nakanuki, Tsuchiura, Ibaraki, 300-0006, Japan*

[*] corresponding author: nomura.shun@jamstec.go.jp

Abstract.

Concrete is widely used in large-scale construction of submarine infrastructure because of its high strength, durability, and ease of handling. However, knowledge of its durability in deep seawater is lacking. In the deep sea, materials are exposed to high pressures and low temperatures, which may cause early deterioration of concrete over time. Concrete materials may also be affected by the chemical composition of seawater, which induces the leaching of calcium. In situ exposure tests are therefore important for understanding degradation processes in the deep sea. In this study, Portland cement based concrete specimens were placed at a depth of 3520 m on the northern edge of the Nankai Trough in 2018 and retrieved in 2019, in the deepest exposure testing conducted to date. Here we provide an outline of the tests, describe the physical properties of materials exposed to deep seawater, freshwater, and air, and discuss possible concrete degradation mechanisms.

Keywords: Deep sea, exposing test, physical property.

1. Introduction

The deep sea is regarded as the 'last frontier' and has attracted much attention in Earth science [1–3]. Recent studies have indicated that the deep sea has potential for the production of natural resources and oceanic energy. There is also interest in the monitoring of ocean-bottom dynamics and management of subsea disasters [4]. Carbon dioxide capture and storage under the seafloor may lead to further utilization of sea-bottom areas [5]. Submarine infrastructure with long-term stability is essential for increasing resource productivity and improving monitoring accuracy.

Concrete is the most preferred material for infrastructure construction because of its cost-effectiveness and rigidity. However, there may be problems with its use in the deep sea, with existing field data being available for depths of up to only 200 m, and with concerns over the durability of concrete in deep-sea environments. Concrete strength may decrease due to the effects of extremely high hydrostatic pressures and low temperatures. Chemical reactions in the deep-sea environment must also be considered. The carbonate compensation depth (CCD) of the Pacific Ocean is of the order of 3000 m. Below that depth, calcium-one of the main components of concrete-may be leached from concrete, promoting its degradation. There may also be other factors, which together affect the durability of concrete in the deep sea. However, the field data concerning concrete properties in the deep sea are lacking, and there are concerns in extrapolating from shallow-water data. Deep-sea exposure testing was therefore undertaken in this study. Here we describe the testing of ordinary Portland cement based concrete specimens at a depth of 3520 m in the Nankai Trough, Pacific Ocean, in the deepest concrete testing yet undertaken.

2. Method

Research cruises were undertaken in 2018 and 2019 as described below.

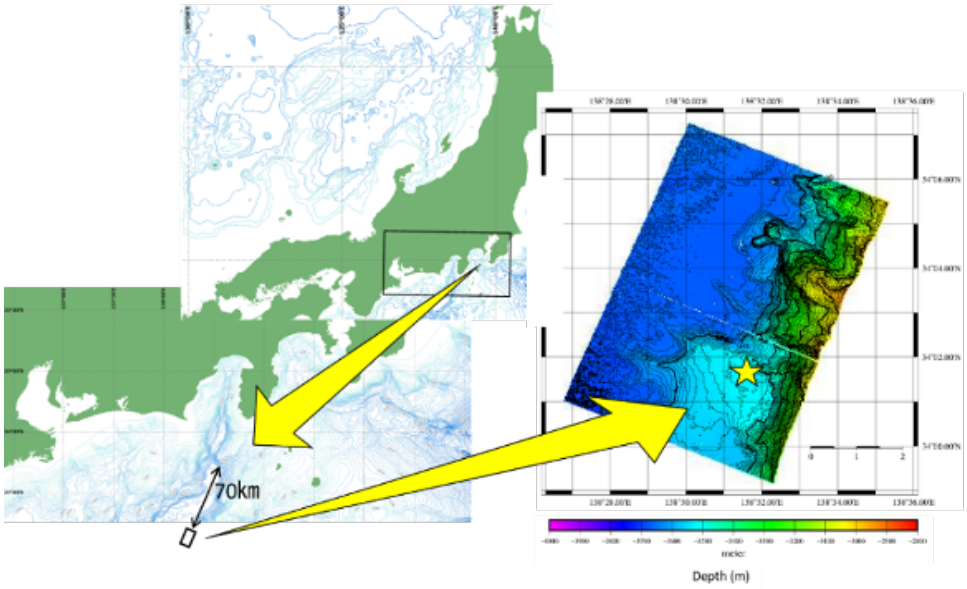

Figure 1. Field location.

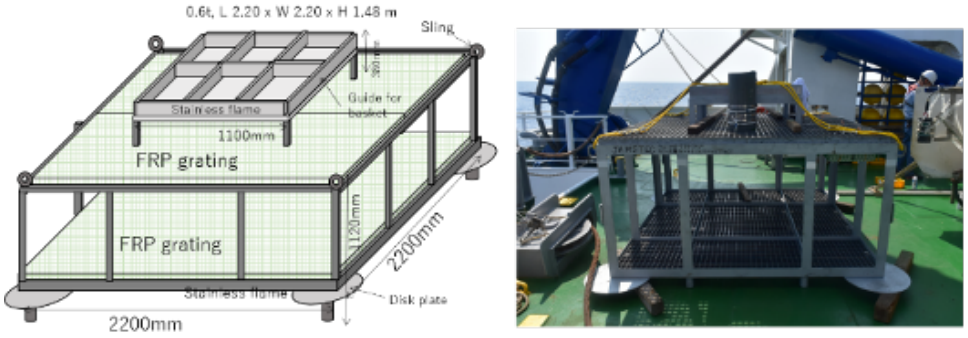

Figure 2. Concept (left) and image (right) of the platform.

2.1. Field location

The concrete exposure area lies on the northern edge of the Nankai Trough, off Sagami Bay, Japan, at 34°1.65'N 138°31.50'E (Figure 1).

Multi-beam echo-sounder (MBES), bathymetric, and bottom-imaging data were obtained by the research vessel 'YOKOSUKA' at locations satisfying the following conditions: depth > 3000 m (below the CCD); ease of access (within a two-day cruise), maximum eight-hour dive, solid seabed, and stable tidal systems.

2.2. Specimen placement

A stainless-steel platform (2.2 × 2.2 × 1.5 m; 600 kg weight) was installed to mount specimens on and to reduce effects of benthic organisms and loss in the strong bottom current (Figure 2). The platform was based on four 200-mm diameter discs to prevent sinkage in the sediment. On 18th July 2018, the platform was lowered from the 'YOKOSUKA' by winch at 45 m.min^{-1}. Concrete specimens (36) were placed in six plastic baskets (400×272×300 mm; Figure 3). Specimen size was 100 mm diameter by 200 mm length (to fit basket pockets). On July 19th, the specimens, in the baskets, were installed on the platform using the deep-sea submersible research vehicle, 'Shinkai 6500', as shown in Figure 4.

2.3. Retrieval of specimens

On 29th September 2019, the study area was accessed by the research vessel 'KAIREI,' and the remotely operated vehicle 'KAIKO' was used to retrieve the specimens after 437 days of exposure. The overview of the research cruises in 2018 and 2019 is presented in Figure 5.

3. Materials and exposure results

3.1. Preparation of concrete specimens

The concrete mix used for the specimens is described in Table 1. Ordinary Portland cement (density 3.15 g cm^{-3}) was used with a water/cement ratio of 0.55. Natural sand (density 2.64 g.cm^{-3}) and crushed limesand (density 2.66 g.cm^{-3}) were mixed and used as a fine aggregate. Coarse aggregate was prepared from crushed limestone (5 − 15 mm particles, density 2.67 g.cm^{-3}; 15 − 20 mm particles, density 2.70 g.cm^{-3}). Admixtures included an Air Entraining Agent (i.e.,

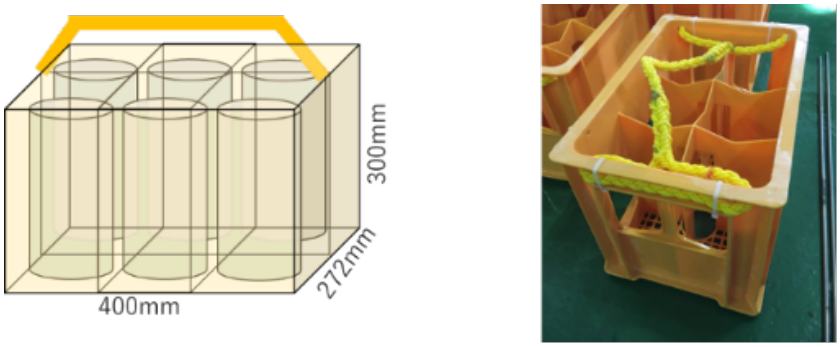

FIGURE 3. Concept (left) and image (right) of the plastic basket the for concrete specimen.

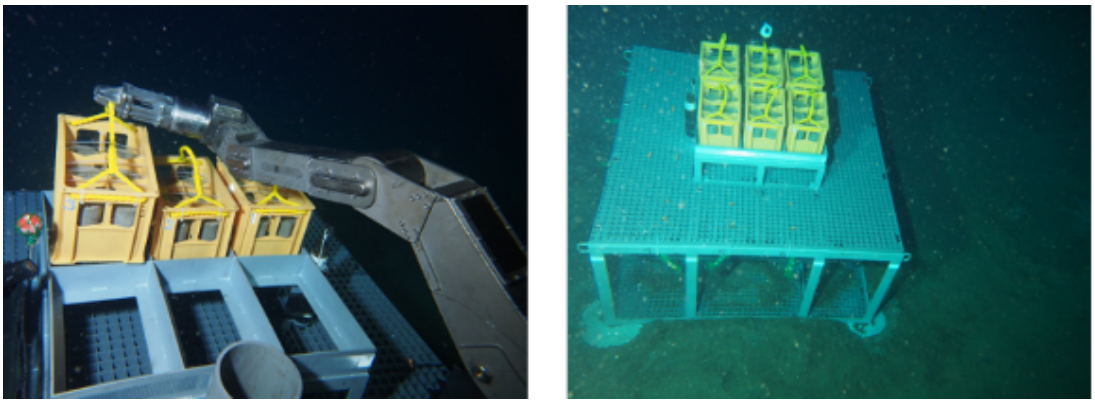

FIGURE 4. Installation of the basket by the manipulator (left) and top view of the exposure system (right).

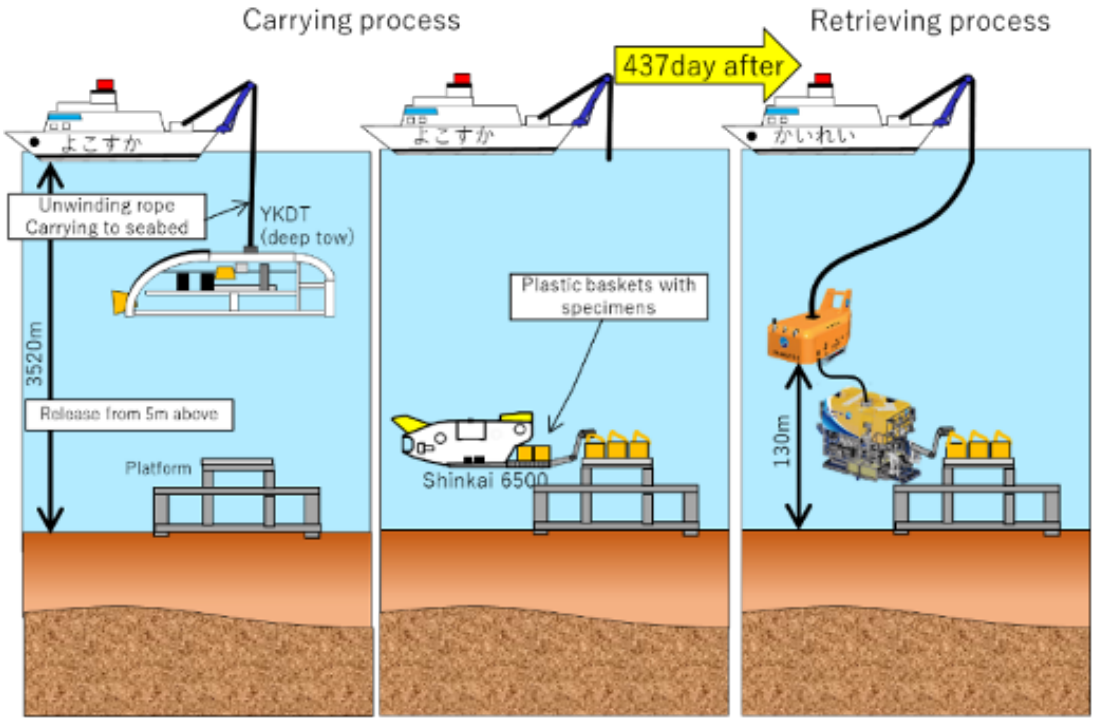

FIGURE 5. Overview of placement and retrieval processes in 2018 and 2019.

Unit content [kg.m^{-3}]								Admixture	
W/C	s/a	W	C	S		G		AE agent	Water reduction agent
[%]	[%]			Lime sand	Natural sand	$5-15$ mm	$15-20$ mm	[A*]	[C × %]
55.0	41.0	157	285	230	532	553	559	3.5	$0.05 \sim 0.2$

* 1A = 0.001%

Table 1. The concrete mix.

Figure 6. Specimens retrieved from the deep sea.

	Deep sea	Water	Salty water
Exposing term		437 days	
Number of specimens	3	2	2
Compression strength f_c (Mpa)	35.4	33.0	39.3
Maximum strain e_a (1E-3)	1.89	1.62	1.70
Young's modulus E_s (kN/mm^2)	22.1	30.5	35.4

Table 2. Averaged compression test values.

AE) agent and a water reduction agent. The slump and air content of the fresh concrete were 8.5 cm and 4.7%, respectively.

The cast specimens were solid cylinders($\varnothing 100 \times 200$ mm) left in the formwork for 1 day before curing in a water bath for 28 days. The water-cured specimens were covered with polypropylene sheet to prevent drying and stored at room conditions pending use. Exposure tests were also undertaken in fresh water and salty water under atmospheric pressure.

3.2. Description of degraded specimens

Recovered specimens are shown in Figure 6. There were no obvious cracks affecting the overall specimen structure. Exposed aggregate was evident on specimen surfaces. There were several spreading white circular spots of $1-3$ cm diameter. The mass density increased by $\sim 1\%$ during exposure, but specimen dimensions were almost the same as after curing for 28 days.

3.3. Compression testing

One-dimensional compression test results obtained by a Hi-ACITS-3000 (Marui & Co. Ltd., Japan) Automatic Compression Testing Apparatus are shown in Figure 7, where profiles represent results of deep-sea, fresh, and salt water. Averaged physical data for the tests are given in Table 2. The deep-sea specimen plot has a lower gradient than that of the other cases, indicating a lower elastic modulus. Compression strengths ranged from 33.0 to 39.3 MPa with small variations, regardless of exposure state, with the maximum strain at the compression strength being the highest for the deep-sea specimens. The Young's modulus values of the deep-sea specimens were $\sim$ 67% of that of the specimen exposed to salt water. The relationship between compression strength and Young's modulus is depicted in Figure 8 where solid and dotted lines represent the upper and lower criteria for materials used in the construc-

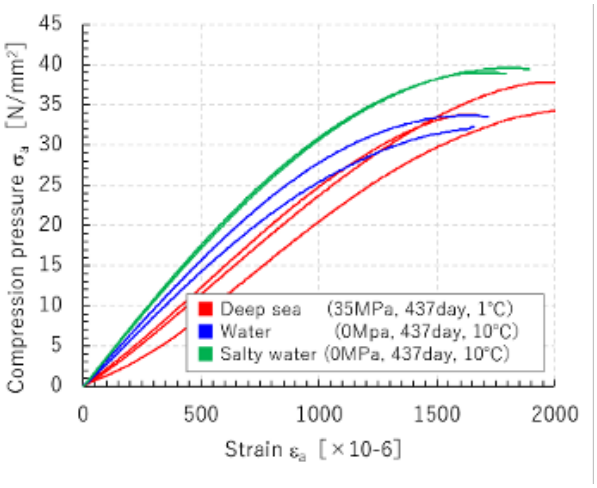

FIGURE 7. Results of compression testing.

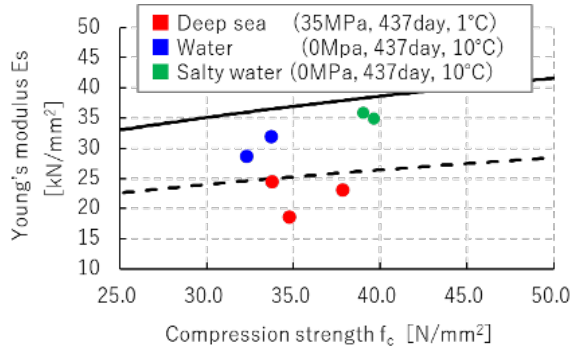

FIGURE 8. Relationship between compression strength and Young's modulus.

tion of buildings and bridges, among others, set by the Architectural Institute of Japan [6]. All deep-sea specimens plot below the lower limit, meaning these specimens were sufficiently degraded to fall short of architectural criteria.

3.4. Travel velocity of ultrasound

Ultrasound travel velocity, VP, was determined using a Pangit PL-200 (FTS Ltd., Japan) instrument, with results as shown in Figure 9. The deep-sea specimens exhibited a decrease in VP relative to the other specimens (18% less than that of salty-water specimens). Based on elastic wave theory, Poisson's ratio ν is expressed as:

$$\nu = \frac{1 - a + \sqrt{|9a - 1||a - 1|}}{4a}, \quad \text{where} \quad a = \frac{V_P^2 \rho}{E_d} \quad (1)$$

where, $\rho[\mathrm{kg.m^{-3}}]$ is density, and $E_d\left[\mathrm{kg.m^{-1}.s^{-2}}\right]$ is the dynamic viscosity coefficient. Figure 10 shows the ν values of specimens exposed to fresh and salt water, representing the general values for concrete materials ($\nu = \sim 0.25$) [7]. In contrast, the lower V_P value of deep-sea specimens ($\nu = \sim 0.39$) is similar to that of non-compressive material ($\nu = \sim 0.50$).

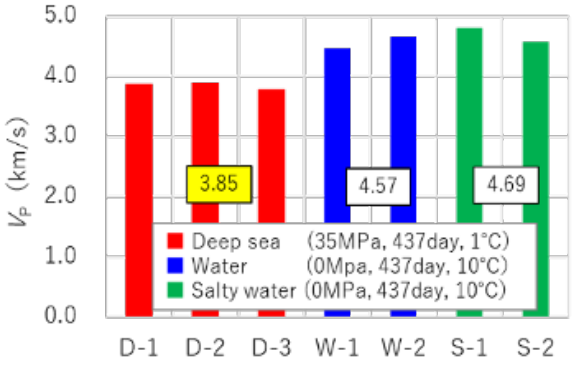

FIGURE 9. Ultrasound travel velocity. X-axis represents the exposure conditions and number of specimens.

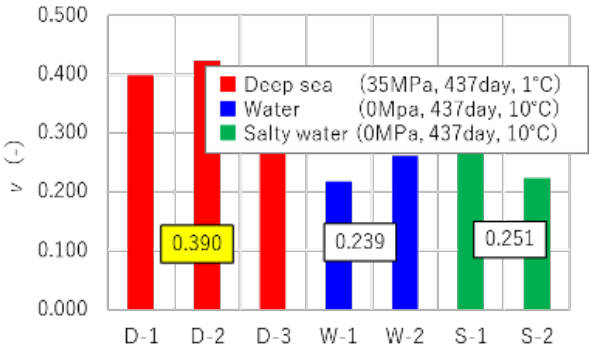

FIGURE 10. Poisson's ratio ν. X-axis represents the exposure conditions and number of specimens.

4. Discussion

The compression and ultrasonic tests confirm that the mechanical states of concrete specimens exposed in the deep sea were different to those exposed to fresh and salt water, with the deep-sea specimens being more ductile and softer. A conceptual representation of the deep-sea exposure environment is provided in Figure 11, illustrating how specimens underwent rapid isotropic loading and unloading (0-35 MPa) during emplacement and retrieval. The specimens were also exposed to high pressures and low temperatures (1−2°C) after installation. It, therefore, seems that the specimens were degraded by short-term mechanical and long-term chemical actions.

To elucidate high loading and unloading effects, Cui et al. [7] performed compression tests after exposure of deep-sea samples to high hydrostatic pressures of 30-500 MPa. They confirmed that as hydrostatic pressure increases, the compressive strength decreases, the strain at compressive strength increases, and the Young's modulus decreases. It was also confirmed by scanning electron microscope (SEM) observations that, even in an isotropic environment, anisotropy develops inside the concrete specimens due to extremely high pressure, with fine cracks developing in the damaged concrete, which had a Poisson's ratio of almost 0.4. These results are consistent with

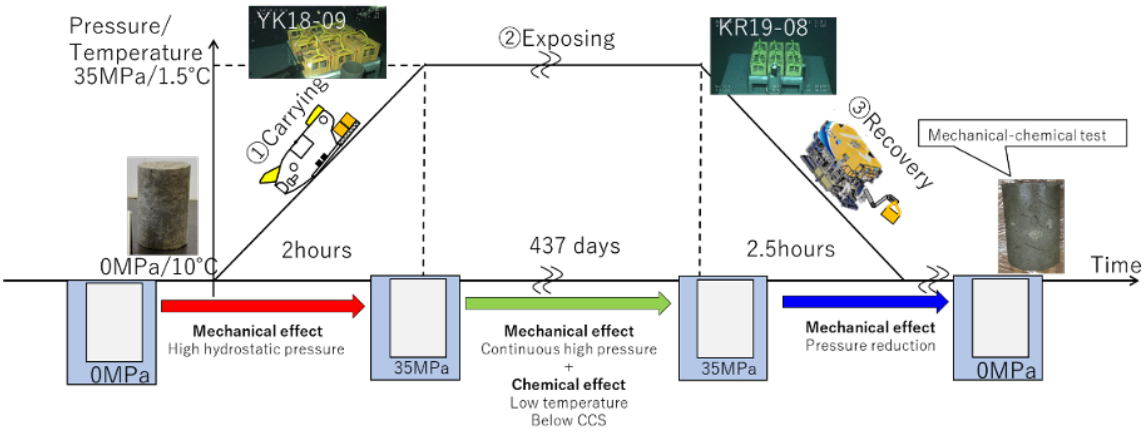

Figure 11. Conceptual representation of the physical and chemical environments around in the concrete specimens.

those for the deep-sea specimens, suggesting that differences in mechanical history contribute to the deterioration of concrete.

5. Conclusion

Concrete specimens were exposed at a depth of 3520 m for 437 days and their physical properties studied. The specimens deteriorated in the deep-sea environment. In this study, we introduced only those physical properties shown by the compression and ultrasonic tests, whereas the deterioration mechanisms are currently being elucidated by mercury injection tests, SEM, electron microprobe analysis, and X-ray diffraction studies. These studies will aid the understanding of physical and chemical processes that affect concrete in deep-sea environments more precisely. Further samples are scheduled to be collected over the next five years, and the scientific reasons for their deterioration may become clearer.

Acknowledgements

We thank Dr Hide Sakaguchi and Mr Masahiko Kamei at Japan Agency for Marine-Earth Science and Technology and Prof. Kenji Kaneko of the Hachinohe Institute of Technology for their useful discussion, research assistance, and encouragement.

References

[1] E. Araki, D. M. Saffer, A. J. Kopf, et al. Recurring and triggered slow-slip events near the trench at the Nankai Trough subduction megathrust. *Science* **356**(6343):1157-60, 2017. https://doi.org/10.1126/science.aan3120.

[2] R. Sharma. Environmental Issues of Deep-Sea Mining. *Procedia Earth and Planetary Science* **11**:204-11, 2015. https://doi.org/10.1016/j.proeps.2015.06.026.

[3] K. A. Miller, K. F. Thompson, P. Johnston, et al. An Overview of Seabed Mining Including the Current State of Development, Environmental Impacts, and Knowledge Gaps. *Frontiers in Marine Science* **4**, 2018. https://doi.org/10.3389/fmars.2017.00418.

[4] W. O. McCarron. Deepwater foundations and pipeline geomechanics, Florida: J. Ross Publishing, pp. 336, 2011.

[5] S. M. Benson, F. M. Orr. Carbon Dioxide Capture and Storage. *MRS Bulletin* **33**(4):303-5, 2011. https://doi.org/10.1557/mrs2008.63.

[6] Reinforced concrete structure calculation standard and explanation, 9th edition, (Tokyo: Architectural Institute of Japan).

[7] J. Cui, H. Hao, Y. Shi, et al. Experimental study of concrete damage under high hydrostatic pressure. *Cement and Concrete Research* **100**:140-52, 2017. https://doi.org/10.1016/j.cemconres.2017.06.005.